Theory of Satellite Structures on Spectral-Line Profiles*†

Ahmet K. Atakan and Harry C. Jacobson
Department of Physics and Astronomy, The University of Tennessee, Knoxville, Tennessee 37916
(Received 25 September 1972; revised manuscript received 15 January 1973)

Theoretical line-shape calculations, which employ an approximation to the classical theory, are compared with experiment to demonstrate that the main features of the satellite-band problem—the line, the high-intensity red satellites, and the blue satellite—can be described simultaneously using simple intermolecular potentials. The comparisons focus on the cesium resonance transitions for which all of the characteristic satellite structures have been observed. In particular, illustrative calculations are detailed for cesium-xenon systems at relative densities of 5–41 and for cesium-argon at 61, and these results are correlated with experiments performed at lower relative densities. The results indicate that widely different potentials can give very similar line profiles. Ancillary conclusions are presented about the role of Lennard–Jones potentials in line-shape calculations.

I. INTRODUCTION

The problem of satellite-band formation on spectral-line profiles has intrigued experimental and theoretical physicists for over 45 years. Extensive observations have been made on the satellities appearing in absorption and emission on the principal-series lines of the alkali metals pressurized by inert gases.[1–3] These features have also been observed on lines in the sharp, diffuse, and fundamental series of the alkali metals[4] on forbidden lines in the alkali metals,[5] and with other absorbers and emitters such as mercury,[6] thallium,[7] indium,[7] the alkaline earths,[8] and the inert gases themselves.[9] The satellites are induced not only by the inert gases but also by perturbers such as H_2, D_2, N_2, and many hydrocarbons.[10]

The resonance lines of cesium contain all of the characteristic satellite structure and the focus here will be on these thoroughly studied transitions. However, the conclusions should be applicable to all of the systems mentioned above. The features for which theory must account are the simultaneous appearance of (a) the shifted broadened line; (b) a high-intensity satellite which appears on the long-wavelength side of the resonance lines in the presence of xenon and krypton but not the lighter inert gases, a satellite which becomes as intense as the line itself at high perturber pressures, (c) a series of low-intensity (perhaps 5%) satellites, also in the red wings, some of which appear to converge and some of which do not[3,11]; and (d) a blue satellite (higher frequency) on the $^2P_{3/2}$ component for each inert gas. Structure has been observed on this blue satellite and frequently two satellites are reported.

A variety of explanations have been published in an effort to account for the individual features of the satellites.[12] These computations propose that red and/or blue satellites arise from transitions between bound states of the Cs–inert-gas molecule,[13,14] configuration interaction which arises when the operator neglected in the Born–Oppenheimer approximation is included,[15] and transitions occurring at points where the potential-energy curves are parallel,[16] and transitions to final states split by the interaction.[17] Another very attractive explanation is that the blue satellites are a consequence of interferences.[18] Others believe that the blue satellites develop from oscillations in the perturbing atom charge distribution[19] and from collision-induced dipole moments.[1(c)]

A systematic comparison of the various explanations with experiments performed under a variety of conditions was initiated in an effort to construct a consistent model of entire line shapes. The theory which emerged and which is detailed below is thus a composite of the insights of many individuals. The calculations indicate that the main features of the problem, the line, the high-intensity red satellites, and the blue satellite can be described simultaneously. The results also indicate that widely different potentials can lead to very similar line profiles. Ancillary conclusions are presented about the role of Lennard-Jones potentials in line-shape calculations.

II. METHOD

As is the case with all line-shape problems there are two aspects: The quantum-mechanical techniques used to treat the interaction of a perturber with the absorbing or emitting atom, and the statistical procedure employed to account for the presence of a large number of perturbers.

A. Intermolecular Potentials

In the system of interest here, the inert gas in its $^1S_0$ ground state, interacts with the cesium atom in its $^2S_{1/2}$ ground state and $^2P_{1/2}$, $^2P_{3/2}$ excited levels to yield molecular states that are characterized as the $X\,^2\Sigma_{1/2}$, $A\,^2\Pi_{1/2}$, $A\,^2\Pi_{3/2}$, and $B\,^2\Sigma_{1/2}$ levels.[20] Information about the ground state is available

from scattering experiments.[21] Analysis of recent line-shape experiments which measure intensities in the wings of the line has yielded information on the short-range portion of these potentials[2] and calculations of the energies are available.[22] Finally, it has been demonstrated that information about excited states can be inferred in a systematic fashion from line-shape experiments.[23]

There are very few physical systems for which experimental results on ground-state interactions are well represented by a potential of the n-6 form, and the computed potentials for the excited states of the cesium–rare-gas system differ significantly from this form. However, in many situations the parameters in such potentials represent the only information about excited states available at present. As part of the present analysis the systematic determination method (SDM)[23] was used to establish parameters in the n-6 potentials for lines which have strong satellite features in an effort to assess the usefulness of the approximation. It will be clear from the results described below that the Lennard-Jones form cannot describe the intensity observed in the far red wings of the line, nor will the form yield blue satellites that behave properly when the pressure is varied.

B. Line-Shape Theory

The general pressures method[24,25] has been used to compute line shapes. The procedure assumes that collisions are adiabatic, perturbers move independently on curved classical trajectories, and interactions add as scalars. When the derivation is repeated for p adiabatic final states, the total line shape for absorption is

$$F(\omega)=\frac{1}{\pi}\sum_{j=1}^{p}\mathrm{Re}\int_0^\infty C_j(s)\,e^{-i\omega s}\,ds\ , \tag{1}$$

where

$$C_j(s)=e^{-n\varphi_j(s)} \tag{2}$$

and

$$\varphi_j(s)=\{1-\exp[i\int_0^s (V_j(t)-V_i(t))\,dt]\}_{\mathrm{av}}\ . \tag{3}$$

In Eqs. (1)–(3), j refers to the final state in question (e.g., here the $B^2\Sigma_{1/2}$ and $A^2\Pi_{3/2}$ states); $V_{j/i}$ is the potential energy between one perturber and the absorber in the final/initial state; and n is the perturber number density. To evaluate Eq. (3), the potentials are expanded as a power series in time and related to the expansion for the potentials developed from the orbit equation. Terms through t^2 are retained here. With the potentials expressed in terms of the initial conditions, the average is over the radial and azimuthal speeds and intermolecular distance R, weighted by the properly normalized value of

$$\exp[-V_i/kT-\tfrac{1}{2}\,m(v_R^2+v_\varphi^2)/kT]\ .$$

The quasistatic form of Eq. (3) is used where noted. In this event

$$\varphi_j(s)=4\pi\int_0^\infty R^2\,dR\,e^{-V_i/kT}(1-e^{i(V_j-V_i)s})\ . \tag{4}$$

The temperatures used in the calculations are those corresponding to experimental conditions.

Certainly the effects of nonadditivity and of diabatic transitions among the excited levels are present. The results reported below, as well as independent calculations,[26] indicate that these effects do not play a crucial role in the experiments analyzed here.

C. Physical Basis

The thrust of the present calculations is to demonstrate that high-intensity red satellites arise from transitions which occur at fairly large values of R where the slope of the difference potential vanishes, that the blue satellites appear as a result of transitions to the $B^2\Sigma_{1/2}$ level at smaller values of R, and that these features appear, along with the main line, in accord with experiment when the potentials are properly chosen.

The low-intensity red satellites apparently are a consequence of (a) higher-order convolutions of the high-intensity red satellite,[16(b)] or (b) transitions to or from bound vibrational levels,[3,27] or (c) interference phenomena.[18] All three may play a part, but the experimental evidence does not appear adequate at present to make quantitative comparisons. It is perhaps worth noting that the type of calculation reported here would produce the features in (a) or (c) if the required averages did not mask them. Throughout the present extensive calculations we have not been able to produce examples of either.

The structure on the blue satellites apparently arises from the same source as the high-intensity red satellites or interference phenomena. Again the experiments available are not sufficient to distinguish the source. Three examples of the first explanation are shown in Sec. III and again, no examples of interference appeared in the present work.

III. RESULTS

Several elements are common to all of the calculations described here. The ground-state potentials were assumed to be of the Lennard-Jones (12-6) form $V_i=A/R^{12}-B/R^6$, where $A=3.68\times10^{-102}$ erg cm^{12} for Cs-Ar and 12.3×10^{-102} erg cm^{12} for Cs-Xe, and $B=3.30\times10^{-58}$ erg cm^6 for Cs-Ar and 7.90×10^{-58} for Cs-Xe.[21(a)] Relative density (r.d) is defined as the density of perturbers under the given conditions relative to that at 0 °C and 1 atm pressure.

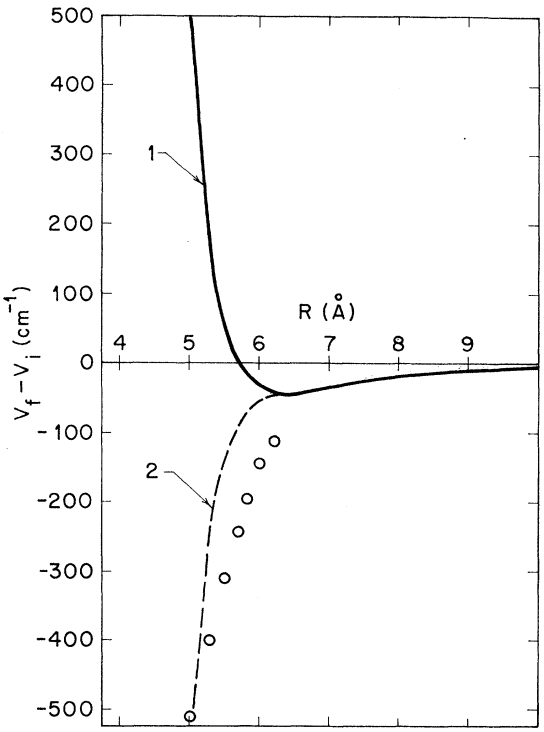

FIG. 1. Intermolecular difference potentials for the $A\,^2\Pi_{3/2} - X\,^2\Sigma_{1/2}$ transition of cesium pressurized by xenon: (solid line) Lennard-Jones (12-6) form; (dashed line) modification of solid line at short range; (circles) data from Ref. 2.

A. High-Intensity Red Satellites

The SDM was used with an experimental line shape observed for the $^2P_{3/2}$ line of Cs perturbed by xenon at a relative density for xenon of 41.3.[28] This line shows no red satellite and as a consequence no information about these satellites was included in fixing the potentials. The difference potential which was inferred is represented by the solid line in Fig. 1 ($V_f = C/R^{12} - D/R^6$, where $C = 54.5\times10^{-102}$ erg cm^{12} and $D = 19.9\times10^{-58}$ erg cm^6). These results were then used in the general pressures theory to compute the lines displayed in Fig. 2, r.d. = 5.0, and Fig. 3 (solid line), r.d. = 9.8. In Fig. 2 the agreement between theory and the observed line and satellite is essentially complete. In Fig. 3 the agreement fails in the far red wings, beyond 100 cm^{-1} or so, when this 12-6 potential is used. The results shown are typical of other calculations performed in the same context.

Two facts speak out against the explanation: Cs-Ar systems have Lennard-Jones difference potentials with minima but high-intensity red satellites are not observed, and the results inferred by Hedges, Drummond, and Gallagher[2] for the $A\,^2\Pi_{3/2}$ state for Cs-Xe are dramatically different (the circles in Fig. 1). (The dashed line in Fig. 1 is within the range of uncertainty of the experiments.) The answer appears to lie in one of two situations, either the averages mask the satellite for the lighter inert gases or, in fact, there is no minimum in the difference potential.

A second complete calculation of the profiles in Figs. 2 and 3 was carried out using the same procedure as that described below for Cs-Xe systems at r.d. = 26.7 and 41.3. Briefly, the total line is given by Eq. (1), with $j = 1$ corresponding to the $A\,^2\Pi_{3/2}$ level and $j = 2$ corresponding to the $B\,^2\Sigma_{1/2}$ level, by Eqs. (2) and (4). The potential differences used are number 2 in Fig. 1, which leads to a line with primarily red components, and that from Fig. 7 which produces a line with both red and blue components. The total lines displayed in Figs. 2 and 3 (and in Figs. 8 and 9) are then the sum of these two results. In Fig. 2 the results are indistinguishable from the general pressures result and in Fig. 3 the dashed line indicates the departure from the general pressure result. The red wing of the computed line at r.d. = 9.8 completes the agreement with experiment in this portion of the spec-

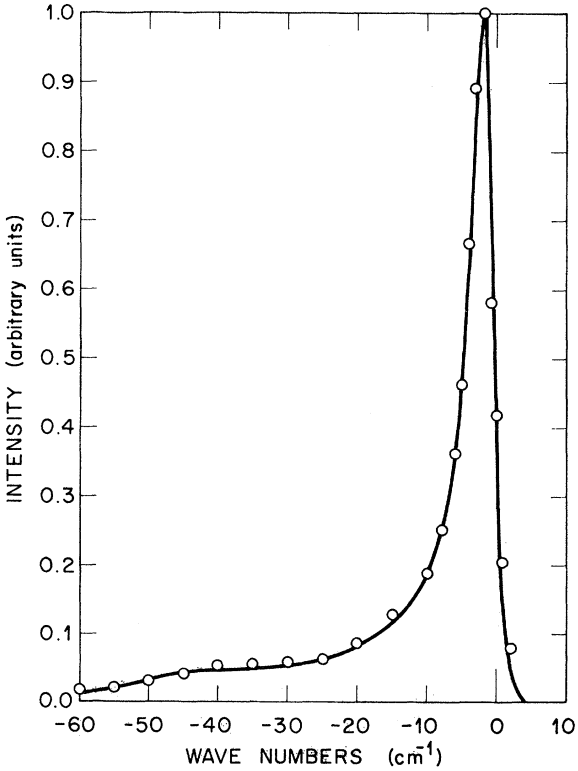

FIG. 2. Comparison of experimental and theoretical line shapes for the cesium $^2P_{3/2}$–$^2S_{1/2}$ transition perturbed by xenon at a relative density of 5.0: (circles) experimental data of Ch'en; (solid line) theory. Temperature $T = 370$ °K.

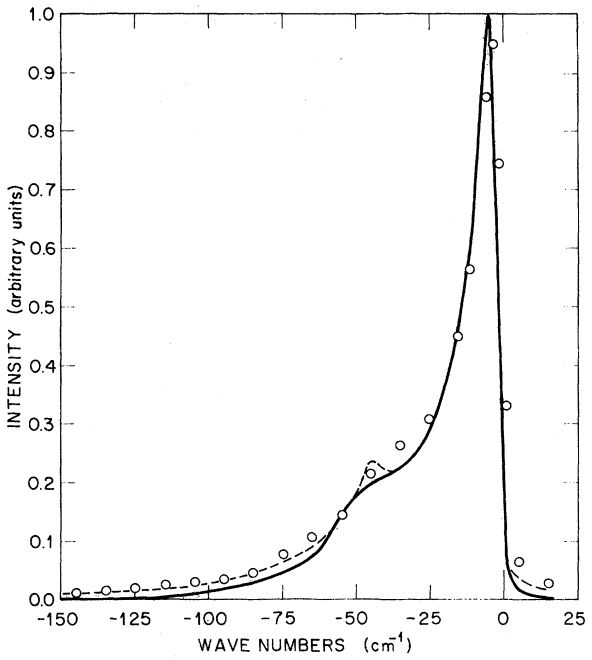

FIG. 3. Comparison of experimental and theoretical line shapes for the cesium $^2P_{3/2}$-$^2S_{1/2}$ transition perturbed by xenon at a relative density of 9.8: (circles) experimental data of Ch'en; (solid line) general pressures result with potential 1 from Fig. 1; (dashed and solid line) quasistatic result with potential 2 from Fig. 1 and potential from Fig. 7. $T = 391$ °K.

trum. (The blue satellite in these experiments is absent at r.d. = 5.0 and begins to appear at r.d. = 9.8; the computed intensity in the blue wing of the line agrees with the observation.)

The results suggest that averages do mitigate sharp features; in the case of light inert gases, the final matching of experimental results which explore short- and long-range portions of the potential may indicate that the difference potential is monotonic everywhere. The results of Figs. 1 and 3 sound one final note of caution: Line-shape calculations can distinguish among alternatives for short-range forms of the potential, but only if accurate comparisons are made many half-widths away from the line center (at least 10 in the present case). Thus potential parameters established from experiments performed where the impact approximation is warranted must be subject to significant uncertainties. This statement is corroborated by our practice of beginning the integration over intermolecular distance at various points to test the sensitivity of computed shapes.

The computed behavior of the satellite is shown for four values of r.d. in Fig. 4. Here the final-state potential is appropriate for the $^2P_{1/2}$ transition ($C = 194.8$ erg cm^{12} and $D = 25.8$ erg cm^6). The potential was obtained with SDM from a line at r.d. = 9.8. The calculations use Eqs. (1)–(3) and are in accord with the observed growth. Tests of the temperature dependence of satellite position and intensity also agree with the facts available.

B. Blue Satellites

Experimentally the blue satellite appears as an extremely weak feature (an intensity of 4×10^{-6} compared to a peak value of one for r.d. = 0.12 of xenon).[29] The feature grows as the perturber density is increased. Experience in observing this growth has led to a rule-of-thumb procedure for decomposing the line and satellite at higher pressures.[1(a)] If the satellite arises from transitions to the $B^2\Sigma_{1/2}$ state it should be possible to use SDM with the decomposed feature to infer a potential. Then the total line shape would be given by Eq. (1) with $j = 1$ corresponding to the $A\,^2\Pi_{3/2}$ level and $j = 2$ corresponding to the $B^2\Sigma_{1/2}$ level. This procedure was explored for both Cs-Ar and Cs-Xe; the following description for Ar is illustrative.

A typical Lennard-Jones difference potential obtained from the satellite is shown as a dashed line in Fig. 5. The excited state is also of this unphysical form, repulsive at large R and attractive at small R. The line shape computed with this potential is shown in Fig. 6 as a dashed line (it is indistinguishable from the solid line in the central region

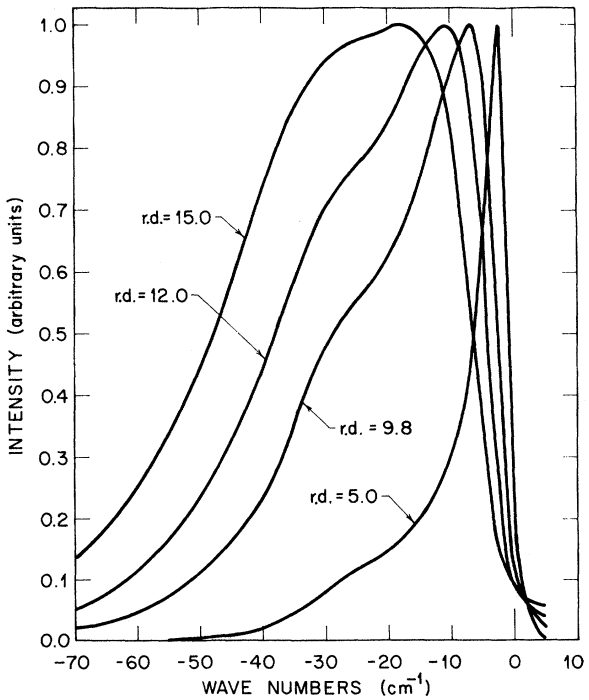

FIG. 4. Computed line shapes at various relative densities for the cesium $^2P_{1/2}$-$^2S_{1/2}$ transition perturbed by xenon. $T = 370$ °K for r.d. = 5.0; $T = 391$ °K for the others.

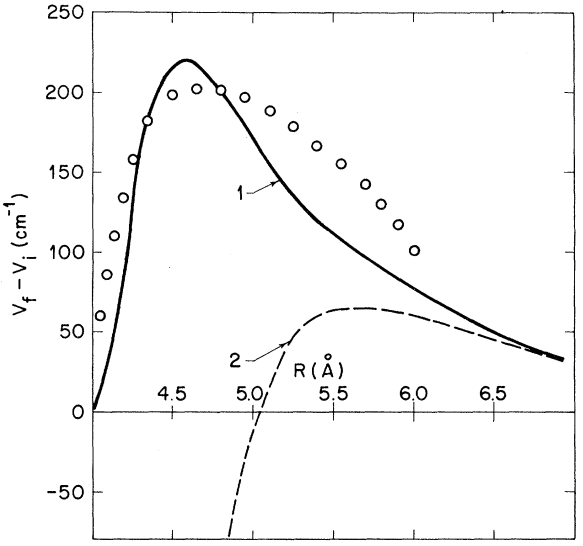

FIG. 5. Intermolecular difference potentials for the $B^2\Sigma_{1/2}$-$X^2\Sigma_{1/2}$ transition of cesium pressurized by argon: (dashed line) Lennard-Jones (12-6) form; (solid line) form with $V_f = 4.66 \times 10^{-58}/R^6$ ergs; (circles) data from Ref. 2.

except at the peak). The result is certainly better than has been reported previously and one might hope that refinements in Eq. (3) would improve the intensity agreement. However, the satellite does not behave correctly in either intensity or position as the relative density is lowered.

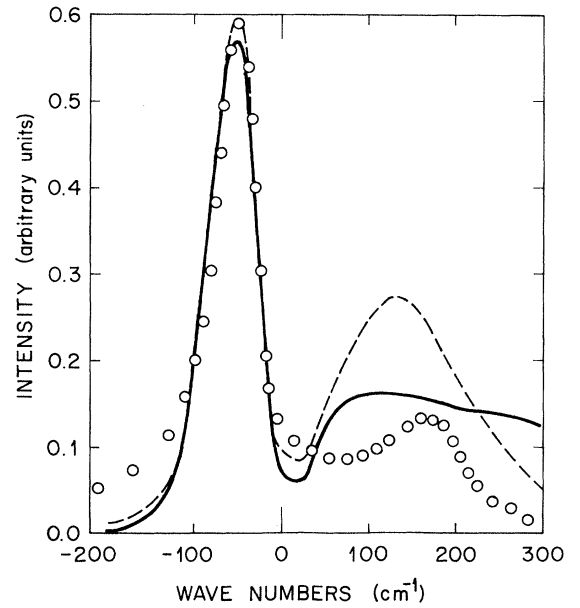

FIG. 6. Comparison of experimental and theoretical line shapes for the cesium $^2P_{3/2}$-$^2S_{1/2}$ transition perturbed by argon at a relative density of 60.8: (circles) experimental data of Ch'en; (solid line) general pressures calculation with potential 1 of Fig. 5 and (12.6) potential for main line; (dashed and solid line) general pressures calculation with potential 2 of Fig. 5 and (12-6(potential for main line. $T = 410$ °K.

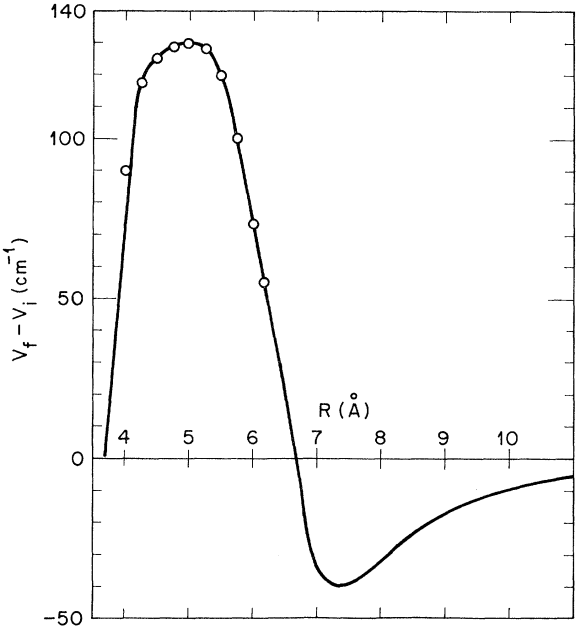

FIG. 7. Intermolecular difference potential for the $B^2\Sigma_{1/2}$-$X^2\Sigma_{1/2}$ transition of cesium perturbed by xenon: (circles) experimental results of Ref. 2.

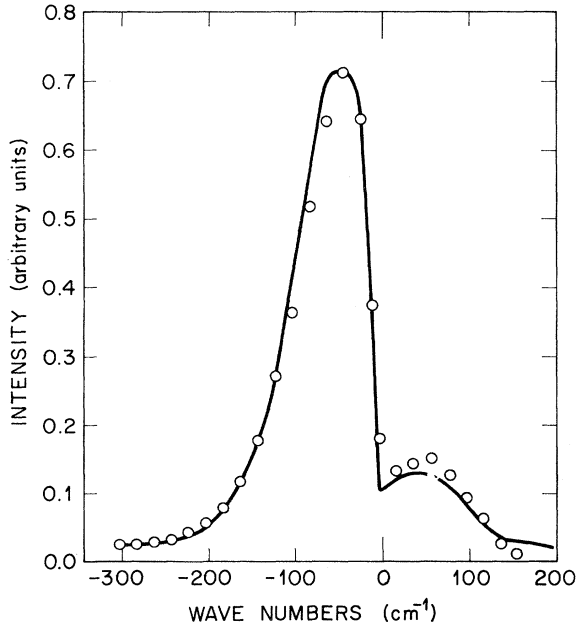

FIG. 8. Comparison of experimental and theoretical line shapes for the cesium $^2P_{3/2}$-$^2S_{1/2}$ transition perturbed by xenon at a relative density of 26.7: (circles) experimental data of Ch'en. $T = 444$ °K.

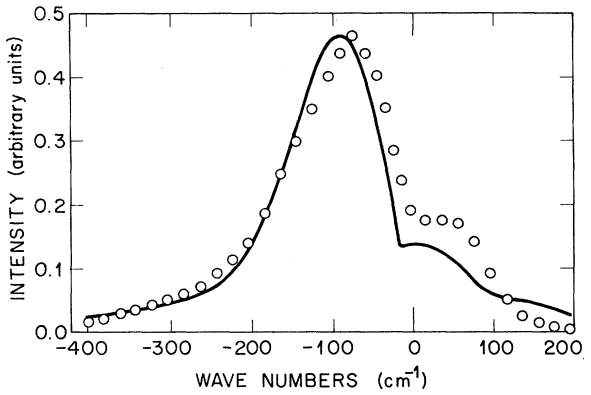

FIG. 9. Comparison of experimental and theoretical line shapes for the cesium $^2P_{3/2}$-$^2S_{1/2}$ transition perturbed by xenon at a relative density of 41.3: (circles) experimental data of Ch'en. $T = 444\,^\circ$K.

The SDM results indicated that the $B^2\Sigma_{1/2}$ potential should be repulsive over a considerable range of R, a fact indicated also by the computed potentials.[22]

The solid curve in Fig. 5 was used with the general pressures method and the line shape shown in Fig. 6 results. The peak intensity is about correct but the calculated satellite is much broader than that observed. Note the structure in the blue wing which is a combination of the ordinary blue-line components and the intensity which arises from the maximum in the difference potential at about 225 cm^{-1}. Also note that the intensity in the red wing computed with a Lennard-Jones (12-6) potential is again well below the observed. (The main line in the figure was computed with $C = 11.37 \times 10^{-102}$ erg cm^{12} and $D = 7.15 \times 10^{-58}$ erg cm^6.) Finally, the very recent experimental results of Ref. 2 have been added as circles in Fig. 5.

Given this background and the belief that the basic explanation is correct, potentials were estimated without making any effort to tailor the potential to reproduce a particular line, and line shapes were computed using Eqs. (1), (2), and (4). The difference potential for the $X^2\Sigma_{1/2} - A^2\Pi_{3/2}$ transition is shown in Fig. 1 (solid for $R \geq 6.45$ Å, dashed for $R \leq 6.45$ Å) while the energy difference for $X^2\Sigma_{1/2} - B^2\Sigma_{1/2}$ is shown in Fig. 7. The circles in Fig. 7 represent experimental results from Ref. 2. The line shapes which result are shown in Fig. 8 for r.d. = 26.7 and in Fig. 9 for r.d. = 41.3. (The results were also displayed for r.d. = 9.8 in Fig. 3.) The red wings are given correctly to -300 and -400 cm^{-1}, respectively. The linewidths and line shifts agree within 20% with those observed. The computed intensity at the peak position of the blue satellite also agrees within 20% with experiment. Note in Figs. 8 and 9 the feature at about 130 cm^{-1} (corresponding to the maximum value of the difference potential, Fig. 7). This intensity arises from the Σ-state difference potential in the same fashion as the high-intensity red satellites since the contribution from Π-state difference potential (Fig. 1) is negligible in this wave-number region.

IV. CONCLUSIONS

The over-all picture provided by these results indicates that good agreement can be achieved between line profile experiments and the theory outlined. The limitations of the calculations, in terms of approximations, potentials employed, and resultant satellite shapes are apparent. The successes of the calculations can now serve as a guide for refinements in the present theory and for comparisons which incorporate quantum-mechanical effects. The comparisons also indicate the need for widely available, accurate, high-resolution intensity measurements over a wide range of perturber densities if we are to sharpen the understanding of potential energies at intermediate values of intermolecular distance, to explore the role of inelastic and nonadditive effects on line structure, and to investigate low-intensity red satellites and the structure on blue satellites.

ACKNOWLEDGMENTS

We are very grateful to Professor S. Y. Ch' en for furnishing the line-shape data which made this analysis possible.

*Work supported by the National Aeronautics and Space Administration under Research Grant No. NGL-43-001-006.

†Based in part on a portion of a dissertation submitted to The University of Tennessee, Knoxville, Tenn., to fulfill a requirement for the Ph.D. degree.

[1](a) D. E. Gilbert and S. Y. Ch'en, Phys. Rev. **188**, 40 (1969); (b) S. Y. Ch'en and M. Takeo, Rev. Mod. Phys. **29**, 20 (1957); (c) R. Granier, Ann. Phys. (Paris) **4**, 383 (1969).

[2]R. E. M. Hedges, D. L. Drummond, and A. Gallagher, Phys. Rev. A **6**, 1519 (1972).

[3]C. L. Chen and A. V. Phelps, Phys. Rev. A 7, 470 (1973).

[4]J. A. Gwinn *et al.*, J. Chem. Phys. **48**, 568 (1968).

[5]F. Besombes *et al.*, Opt. Commun. **1**, 161 (1969).

[6]S. Robin and S. Robin, Rev. Opt. Theor. Instrum. **37**, 184 (1958).

[7]S. Y. Ch'en *et al.*, Physica (Utr.) **27**, 1170 (1961).

[8]S. Y. Ch'en and A. T. Lonseth, Phys. Rev. A **3**, 946 (1971).

[9]M. Castex *et al.*, C.R. Acad. Sci. (Paris) **268**, 552 (1969); R. Granier *et al.*, C. R. Acad. Sci. (Paris) **264**, 778 (1967).

[10]O. Jefimenko and S. Y. Ch'en, J. Chem. Phys. **26**, 913 (1957).

[11]O. Jefimenko and W. Curtis, J. Chem. Phys. **27**, 953 (1957).

[12]It is not possible to reference adequately the development of our present understanding, apart from an extensive review.

Some of the work since the review of Ref. 1(b) is included in the present paragraph.

[13]A. Michels *et al.*, Physica (Utr.) **25**, 1321 (1959).

[14]L. Klein and H. Margenau, J. Chem. Phys. **30**, 1556 (1959).

[15]R. G. Breene, Jr., Phys. Rev. A **2**, 1164 (1970).

[16](a) O. Jefimenko, J. Chem. Phys. **39**, 2457 (1963); J. F. Kielkopf and J. A. Gwinn, J. Chem. Phys. **48**, 5570 (1968); J. F. Kieffer, J. Chem. Phys. **54**, 1852 (1969); M. Takeo, Phys. Rev. A **1**, 1143 (1970); G. D. Mahan, Phys. Lett. A **39**, 145 (1972); Phys. Rev. A **6**, 1273 (1972); (b) W. R. Hindmarsh and J. M. Farr, J. Phys. B **2**, 1388 (1969); R. P. Futrelle, Phys. Rev. A **5**, 2162 (1972), and the extensive references therein; A. Royer, J. Chem. Phys. **50**, 1906 (1969); Phys. Rev. A **3**, 2044 (1971).

[17]R. Herman and L. Herman, J. Quant. Spectrosc. Radiat. Transfer **4**, 487 (1964).

[18]A. Royer, Phys. Rev. A **4**, 499 (1971); F. H. Mies, J. Chem. Phys. **48**, 482 (1968).

[19]Y. Leycuras, J. Quant. Spectrosc. Radiat. Transfer **6**, 131 (1966).

[20]G. Herzberg, *Spectra of Diatomic Molecules* (Van Nostrand, New York, 1950).

[21](a) R. B. Bernstein and J. T. Muckerman, in *Intermolecular Forces*, edited by J. O. Hirschfelder (Interscience, New York, 1967), Chap. 8; (b) C. J. Mallerich and R. J. Cross, Jr., J. Chem. Phys. **52**, 386 (1970).

[22]W. E. Baylis, J. Chem. Phys. **51**, 2665 (1969); and private communication.

[23]H. Jacobson, Phys. Rev. A **4**, 1368 (1971); the method establishes a few parameters from an overdetermined system using least-squares methods on line-shape data; in the present application the parameters in an n-6 form of the excited-state potential are inferred from the experimental results.

[24]A. K. Atakan and H. C. Jacobson, J. Quant. Spectrosc. Radiat. Transfer **12**, 289 (1972).

[25]R. L. Fox and H. C. Jacobson, Phys. Rev. **188**, 232 (1969).

[26]H. C. Jacobson, Phys. Rev. A **5**, 989 (1972).

[27]G. D. Mahan and M. Lapp, Phys. Rev. **179**, 19 (1969); W. E. Baylis, Phys. Rev. A **1**, 990 (1970).

[28]All of the experimental results compared in this paper were furnished by Professor S. Y. Ch'en.

[29]R. J. Exton (private communication).

PHYSICAL REVIEW A VOLUME 7, NUMBER 5 MAY 1973

Double- and Triple-Photon Decay of Metastable $^3P_0$ Atomic States*

Robert W. Schmieder†

Lawrence Berkeley Laboratory, University of California, Berkeley, California 94720

(Received 8 December 1972)

The radiative decay of metastable $nsnp\ ^3P_0$ atomic states is found to occur only by odd-parity multiphoton modes such as $E1M1$ and $3E1$, in the absence of hyperfine structure. A detailed calculation of the $E1M1$ rates for several members of the Be sequence is presented, in the nonrelativistic approximation. Only the general properties of $3E1$ decay are presented. Among other results, the $3E1$ rate is found to be zero if any two photons have the same energy, and its spectrum, unlike the symmetrical two-photon spectra, is found to be irregular and asymmetric, being peaked somewhat below half the transition energy.

I. INTRODUCTION

In most atoms with two valence electrons, such as the Be, Mg, Ca, Zn, and Cd isoelectronic sequences, the lowest excited state is $nsnp\ ^3P_0$. Energetically this state can radiatively decay only to the $nsns\ ^1S_0$ ground state, but owing to the $0 \not\to 0$ selection rule, this transition is strictly forbidden for all single-photon modes. In reality, this transition is observed as a forbidden line in laboratory and astrophysical sources. Bowen[1] suggested that this transition is enabled by the interaction of the electrons with nuclear moments. In isotopes with nonzero nuclear moments, the coupling of the nuclear spin I to the $^3P_0$ state produces a state of total angular momentum $F = I \neq 0$, thus circumventing the $0 \not\to 0$ selection rule. This idea was tested experimentally by Mrozowski,[2] Kessler,[3] and by Deloume and Holmes,[4] who showed that only the odd isotopes produce the emission line. Later calculations by Garstang[5] gave rates for Mg I, Zn I, Cd I, and Hg I. Such calculations assume that the hyperfine structure mixes the $^3P_0$ and $^3P_1$ states, and that spin-orbit and spin-spin interactions mix the $^3P_1$ with $^1P_1$ states, thus enabling the $^3P_0 \to {}^1S_0$ transition to occur in the electric dipole ($E1$) mode.

In even isotopes, this mechanism is not possible—no single-photon decay can occur. We must, therefore, consider multiphoton modes, for which $0 \to 0$ is allowed.

Two-photon decay has been studied several times in the past. In atoms, the $2S \to 1S$ transitions in hydrogenlike and heliumlike ions occur primarily by the $E1E1$ (or $2E1$) mode, and theory and experiment are in good agreement.[6] A recent calculation by Johnson[7] gave relativistic results for the $2E1$ rate of the $2\,^2S_{1/2} \to 1\,^2S_{1/2}$ transition of hydrogenlike ions, and an estimate of the $2M1$ rate. Eichler and Jacob[8] have derived general properties of $ELEL'$, $ELML'$, and $MLML'$ modes, and Grechukhin[9] has extended these calculations and applied them to nuclear transitions. Experimental